A COMPACT, LOW JITTER, FAST RISE TIME, GAS-SWITCHED PULSE GENERATOR SYSTEM WITH HIGH PULSE REPETITION RATE CAPABILITY*

Ronald J. Focia[ε]
RF Engineering/Pulsed Power Laboratories, Inc., PO Box 429
Edgewood, NM 87015 USA

Charles A. Frost
Pulse Power Physics, Inc.
Albuquerque, NM 87122 USA

Abstract

We present the experimental results of an ongoing research effort focused on the development and refinement of a compact, low jitter, fast rise time, command triggered, high peak power, high pulse repetition rate (PRR), gas-switched pulse generator system. The main component of the system is a gas-switched Marx-like pulse generator module designed for applications including UWB radar, microwave sources, and triggering large scale multi-module pulsed power systems of all types. The pulse generator system, comprised of a single or multiple Marx modules, is command triggered by a single or multiple TTL level pulses generated by a timing and control system implemented using LabVIEW software and a PXI-based hardware system. The TTL trigger pulses fire all solid-state high voltage trigger pulsers that close the first stage switches in the Marx modules using a novel method to reduce jitter. The control system also accepts user input to set the desired output conditions, adjusts the charge voltage of a high voltage capacitor charging power supply, inhibits capacitor charging during firing of the pulse generators, and can control the system in a closed-loop fashion to maintain relative timing and output characteristics during timing drifts and changing environmental conditions. The individual Marx stages are compact and stackable and utilize field enhanced spark gap switches. The stage capacitors are charged in parallel through mutually coupled inductors in series with resistors. This charging scheme allows for high PRR operation limited only by the stage switch recovery time and the power of the available capacitor charging power supply. The stage switches are optically coupled to aid in Marx output voltage formation and to minimize system jitter. The Marx generator is housed in a lightweight aluminum pressure vessel and is operated in a low pressure dry air environment. The design exhibits a low inductance which varies depending on the number of stages used. Using a five stage prototype, we have generated output voltages of ~100 kV with a rise time of <4 ns. The output pulse width is variable and is dependent on the value of the Marx stage capacitors used and the load resistance. The pulse generator system has been operated in a burst mode at a PRR in excess of 1 kHz with good output voltage regulation. The total jitter of the Marx generator system, i.e. from the application of the trigger pulse to arrival of the output pulse, was measured and found to be <1 ns.

I. INTRODUCTION

This paper summarizes the current status of a Phase II Small Business Innovation Research (SBIR) effort funded by the Air Force Research Laboratory, Directed Energy Directorate. The solicitation for the Phase I topic (SBIR 04.1, topic A04-009) called in general for high pulse repetition rate (PRR) pulsed power generators. The choice of technology for a solution to the problem and the operating design goals were left open to suggestion. When formulating our Phase I plan of action, we studied the literature available on the subject and devised a solution that combined the best ideas from multiple independent experiments and our own new ideas in order to provide a unique solution to the problem. Our efforts were successful and led to award of a Phase II project. The Phase II results to date are summarized in the following paragraphs.

We feel that the work presented here is unique. In Phase I we designed a gas-switched Marx generator that can be operated at a PRR in excess of 1 kHz in burst mode. In Phase II the system design was revised to allow for a configurable output polarity from a single charging voltage polarity, a lower overall inductance, and low total system jitter. A dual-triggered trigatron scheme was devised that allows for sub-nanosecond trigger to output jitter and synchronization of multiple pulse generators.

* This work was supported AFRL, Directed Energy Directorate, under contract number FA9451-05-C-0021.
ε email: rfocia@pulsedpwr.com

II. SYSTEM OVERVIEW

The Phase I research effort focused on using a gas-switched Marx generator design to provide the desired output voltage levels. In Phase II, the design was refined to allow for better overall performance. The key features of the Phase II design are:

- A compact, lightweight, and portable design that is housed in a tubular containment pressure vessel,
- A configurable output polarity using a single polarity charging source,
- A modular construction that allows setting the output voltage and pulse width as desired,
- Utilization of corona-stabilized (or field enhanced) spark gap switches for high PRR operation [1],
- Optical coupling of spark gap switches to reduce system jitter,
- A triggering scheme that allows for a sub-nanosecond command trigger to output jitter, and
- Parallel resonant charging using a series inductance and resistance in each stage to support high PRR operation.

The tubular containment pressure vessel is shown in Figure 1. The outer diameter at each end flange is 127 mm. Each flange has a removable, O-ring sealed cover plate installed which is held in place by six Allen head cap screws. The main tube inner diameter is 102 mm. The inner length of the containment vessel is 406 mm which allows for housing a design maximum of ten Marx stages with some room left over for additional components, such as a peaking switch, if desired. The overall length of the vessel is 460 mm. If loaded with all ten stages, the total weight of the Marx generator is 5.3 kg. The physical attributes of the pressure vessel make it a highly compact and portable system.

Figure 1. Tubular containment pressure vessel.

All connections to the Marx generator are made through one flange cover. In the standard configuration, the protrusions through the flange cover are for pressurized gas inlet, high voltage for capacitor charging, high voltage output, trigger inputs, and B-dot probe outputs. The metal pressure vessel acts as the ground reference. A Teflon liner is installed on the inside of the pressure vessel to mitigate high voltage arcing. The output of the Marx generator folds back through the center of the stages in order to minimize inductance.

The Marx generator is designed to work using dry air as the pressurizing gas. Other gasses have been evaluated. However, dry air provided the best performance at high PRR operation. Portable operation is easily accomplished using a scuba tank as the source of pressurized air.

Each stage of the Marx generator is designed for a 20 kV maximum charge voltage. The design uses a single positive polarity charging voltage and the stages can be configured to provide a positive or negative polarity output voltage. The design accommodates a maximum of ten stackable stages. Each stage can have various types and sizes of capacitors installed to achieve the desired output characteristics. Each stage capacitor is charged in parallel through a series resistance and inductance with mutual coupling as elaborated on by Baum and O'Loughlin.[2,3] For high PRR operation, a high power charging supply must be used. For low PRR or portable operation, a high voltage DC-DC converter can be used to charge the stage capacitors.

Each stage of the Marx generator can be stacked together and the stack plugs into a base plate that is mounted to the flange cover. Once the stack is assembled on the flange cover, it slides into the Teflon lined pressure vessel. The capacitance in each stage and number of stages is variable and can be set to achieve the desired pulse width and output voltage magnitude.

The output connector is a pressure sealed re-entrant type. Two types of coaxial cable can be accommodated using different size re-entrant connectors depending on the maximum output voltage that the Marx generator is configured for.

Low jitter triggering of the Marx generator requires a bipolar trigger input. The low jitter triggering scheme is described in the following section. For low jitter triggering, the first two stage switches are needed and the minimum number of stages is three. If low jitter triggering is not required, only the first stage switch is triggered and the minimum number of stages can be set at two. The solid-state bipolar trigger generators can be powered from 220 VAC or from 12 VDC for low PRR or portable operation.

The Marx generator has two built-in B-dot probes installed to monitor current in the Marx ground return path. The B-dot probes are configured to provide opposite polarity outputs so that common mode noise can be rejected if necessary.

III. LOW JITTER TRIGGERING

The Phase I Marx generator design used a trigatron switch in the first stage and only the first stage switch was triggered. Although the compact, UV coupled, and corona stabilized spark gap design resulted in a relatively low jitter for the Marx generator itself ($\sigma_{RMS} \approx 636$ ps), the jitter from command trigger to output was on the order of several nanoseconds.

One goal of the Phase II effort was to reduce the command trigger to output pulse jitter to <1 ns so that several Marx generators could be synchronized to form a high power array if desired. To achieve this goal, several switch geometries were evaluated, including standard trigatrons with various trigger pin geometries, trigatrons using high-K ceramic materials surrounding the trigger pin, mid-plane triggered field distortion gaps, overvolted two-electrode triggered gaps, and a new type of triggered spark gap that we call the dual-pulsed trigatron design. In the end, the dual-pulsed trigatron design allowed for achieving the desired low trigger jitter goals. This triggering scheme is discussed in the following paragraphs.

Figure 2 shows schematically the new dual-pulsed trigatron switch configuration as it would be employed in the first two stages of a Marx generator. Key to implementation of this method is the use of a solid-state, low jitter, high voltage trigger pulser with a bi-polar output described in a subsequent section.

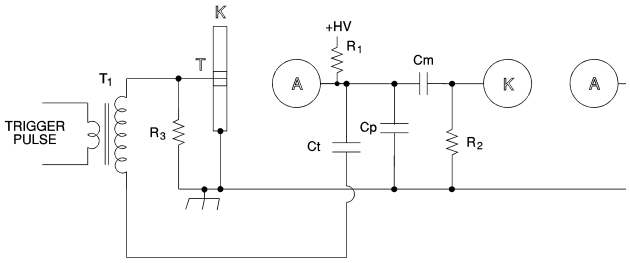

Figure 2. Schematic of the new dual-pulsed trigatron switch configuration.

The circuit in Figure 2 is quite similar to a standard trigatron circuit. However, the positive going output of trigger transformer T_1 is coupled through trigger capacitor C_t to the anode of the first stage switch. When the trigger pulse is first applied, almost the full potential drop occurs across the trigger gap T-K which rapidly breaks down. This is because the capacity of the trigger gap is much smaller than the series combination of capacitors C_t and C_p. When the trigger gap closes, the full transformer potential is rapidly applied to the switch anode and heater capacitor C_p. This circuit achieves a simultaneous UV illumination of gas molecules in the gap and over-voltage of the gap potential. The heater capacitor C_p rapidly heats the discharge channel and switch closure causes the large potential to appear on the cathode of the following stage.

Figure 3 shows the trigger pulse and voltage waveforms across the anode-cathode gap of the dual pulsed trigatron circuit of Figure 2. Separate waveforms show charge voltage on the gap of 0%, 50%, and 80% of the 11.4 kV self-breakdown (SB) voltage. The main gap spacing is 0.05 inches, and operating pressure is 35 psia dry air. The only difference between the physical configuration of this gap and the standard trigatron gap is that the trigger pin is slightly recessed behind the flat surface of the cathode, rather than being flush with it. The data of Figure 3 show that the voltage on the anode starts to rise immediately after the firing of the trigatron gap. For the case with zero initial voltage on the anode, the voltage rises to 50% of the breakdown level in approximately 50 nanoseconds without firing. With 50% of the self-breakdown voltage charging the gap, breakdown occurs near the center of the pulse charging ramp and at a voltage level that is almost 100% of the self-breakdown level. With higher charging voltage the voltage across the anode-cathode gap can actually exceed the self-breakdown before the switch fires. This mode of operation leads to more intense ionization of the channel and reduced resistive phase loss.

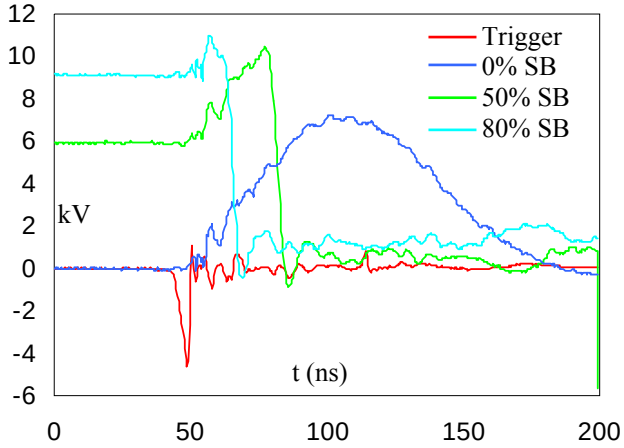

Figure 3. Voltage waveforms across anode-cathode gap of dual-pulsed trigatron for 0%, 50%, and 80% of the 11.4 kV self-breakdown (SB) voltage.

Figure 4 shows the voltage waveforms which would be applied to the cathode of the second stage of the Marx generator circuit in actual operation. This waveform is measured across monitor resistor R_2. The risetime here is substantially faster than for a standard trigatron operating at the same gap spacing and pressure. The over-shoot on the front of the waveform indicates that the resistive phase of switch closure occurs more rapidly, and some inductive resonance ring-up on the waveform is observed. If this switch was driving the second stage, breakdown of the second stage switch would occur in less than 1 nanosecond and with extremely low jitter. This is the desired situation for the low jitter triggering of a Marx generator.

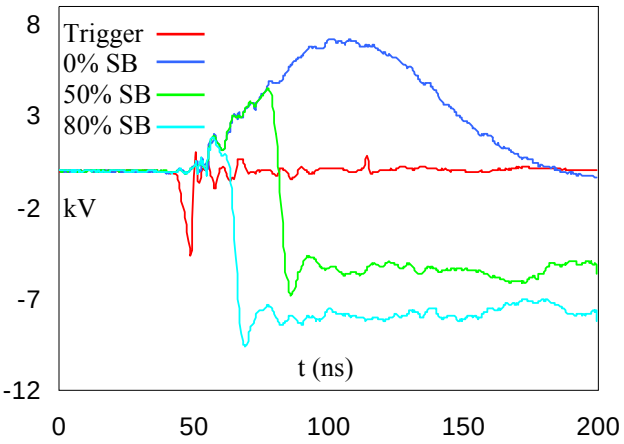

Figure 4. Voltage waveforms at the cathode of the second stage switch when the dual-pulsed trigatron fires.

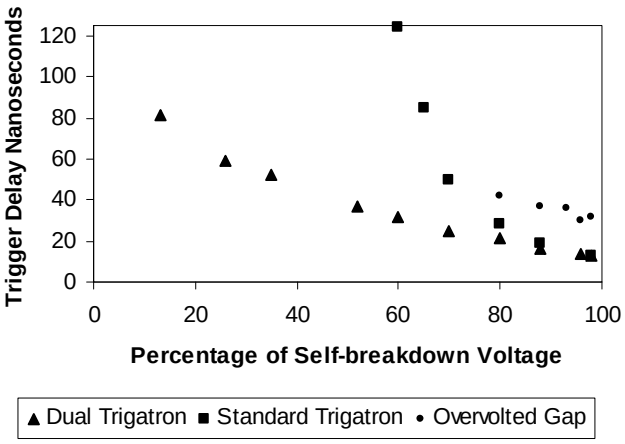

Figure 5. Switch trigger delay measured for three different methods of triggering a trigatron switch with 11.4 kV hold-off.

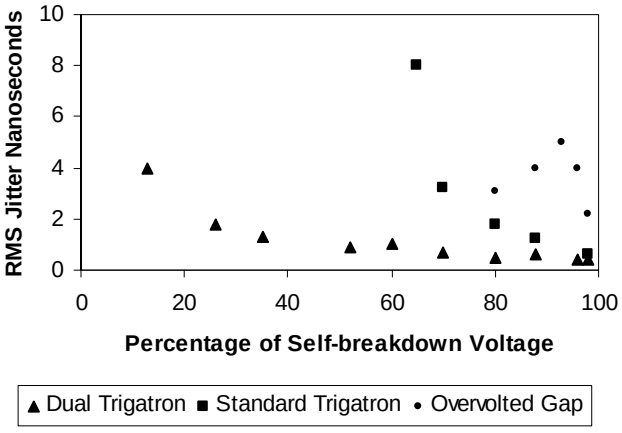

Figure 6. Standard deviation of the trigger delay data shown in Figure 5.

Figure 5 shows the trigger delay measured as a function of charging voltage for three different methods of triggering a trigatron switch. For all three cases the basic geometry and dimensions of the switches are identical with a 0.05 inch anode-cathode gap operating at a pressure of 35 psia. Identical trigger levels were applied to the switches for all cases. For all three cases the switch was operated at a 200 Hz repetition frequency. Data for the new dual-pulsed trigatron is shown by the triangle symbols. The circle symbols show data for an over-volted two-electrode gap without the trigger pin. Comparing the curves it can be seen that the dual-pulsed trigatron design is superior in giving a lower trigger delay and allowing triggering down to 20% of the self-breakdown voltage. The standard trigatron performs well above 90% of self-breakdown but the delay drops rapidly with charge voltage. The over-volted two-electrode gap without UV illumination from the trigger pin gives a greater delay and ceases to trigger below 80% of self-breakdown voltage. The data for the over-volted gap, however, is indicative of what would occur for the non-triggered second stage gap in the Marx generator without the presence of UV illumination from the first stage gap. This data indicates that it is necessary to use UV coupling in the Marx to achieve a low jitter.

Figure 6 shows the standard deviation of the trigger delay corresponding to the data points of Figure 5. Again, each data point represents the average of 64 individual measurements of the time delay, and the RMS jitter value corresponds with one standard deviation from the mean. The data indicate that the new dual-pulsed trigatron design allows triggering with sub-nanosecond jitter when operated at 80% of the self-breakdown voltage. This result meets our requirements for use in the Phase II Marx generator application. The other gap designs show a substantially higher jitter and cannot be triggered at reduced charge voltages.

The effects of changing the gap spacing and operating pressure were investigated in order to optimize performance of the dual-pulsed trigatron design. As anticipated, operation at higher pressures with shorter gap lengths gives the lowest switching jitter. A gap spacing of 40 mils provides a reasonable compromise between performance and switch lifetime.

In order to explore the dual-pulsed trigatron lifetime, we operated the switch for a total of 3.6×10^5 pulses by firing the triggered switch at a constant pulse repetition frequency of 100 Hz for a period of one hour. No noticeable change in the switch risetime or triggering jitter was observed. After the test run the switch was disassembled and inspected. Neither the trigger pin nor the main electrodes showed significant signs of wear. It seems reasonable that this switch design could operate for $\sim 10^6$ discharges between maintenance intervals. This should be more than adequate for most applications. The Marx discharge capacitor C_m employed for these tests had a value of 150 pF. If a larger value of capacitor is used, the lifetime will be reduced proportionate to the total charge passing through the switch.

IV. TRIGGER PULSE GENERATOR

Key to achieving sub-nanosecond trigger jitter in the Phase II Marx generator was development of a bipolar, solid-state, high voltage, and low jitter trigger pulse generator. Several designs were evaluated and prototyped. The final design uses a four-stage semiconductor Marx generator as the primary pulse generator with pulse sharpening provided by a ferrite core magnetic switch.

A simplified schematic of the bipolar trigger pulser is shown in Figure 7. The solid-state Marx generator uses inexpensive consumer-grade IGBT (Insulated Gate Bipolar Transistor) type closing switches. A high resistivity Ni-Zn iron ferrite material was used in the fast magnetic switch. In this application we employed a total of twelve of the IGBT devices in the four-stage Marx generator where three parallel devices were employed in each stage. When combined with a single ferrite core magnetic pulse-sharpening switch, a pulse rise time of approximately 5 nanoseconds was applied to the primary of the pulse transformer. This was transformed to the high voltage level required to match the high impedance capacitive load provided by the triggered switch electrodes.

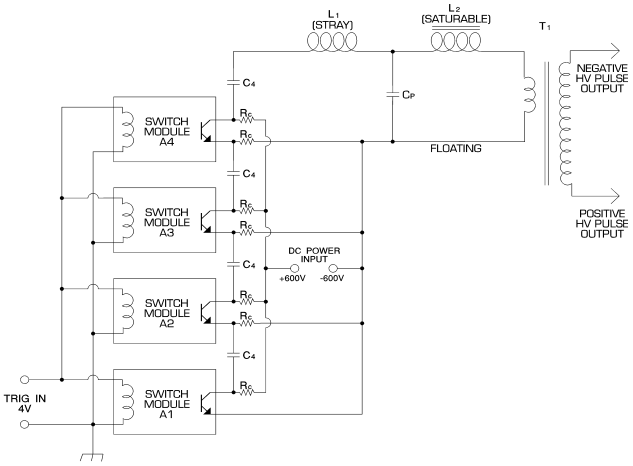

Figure 7. Simplified schematic of the trigger pulser.

The trigger pulser requires +/- 600 VDC input voltage. For high PRR operation, the input voltage is provided by 220 VAC mains converted to DC using a pair of standard half-wave voltage doublers operated in opposite polarity modes. For portable or low PRR operation, a DC-DC converter can be used to provide the required input voltage.

The output parameters of the complete spark gap trigger system were characterized by feeding the differential output voltage from the positive and negative pulser output leads directly to a high-voltage nanosecond-rise time resistive voltage divider probe. The probe output was attenuated with a Barth high-voltage attenuator followed by a standard 50 Ω attenuator. The waveforms were recorded on a Tektronix model TDS3044B digitizer.

Figure 8 shows the measured trigger pulser output voltage waveform. For this waveform the pulser was operated at a sustained repetition rate of 300 Hz and the AC line input voltage was set at 220 VAC. Measured output voltage was 28.1 kV and rise time was 7.3 ns. Time delay through the unit was <20 ns with a statistical triggering jitter of 130 ps.

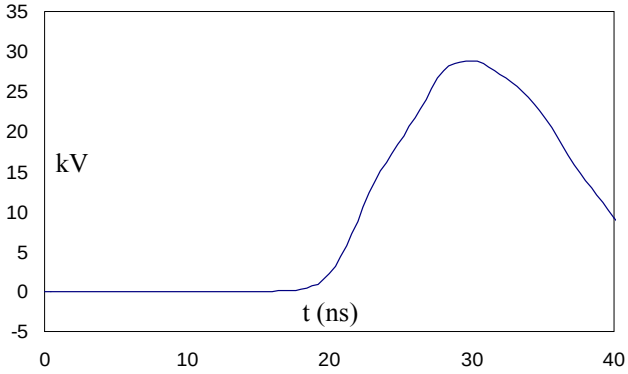

Figure 8. Trigger pulser output voltage waveform.

V. TIMING AND CONTROL SYSTEM

Triggering the Phase II gas-switched Marx generator with sub-nanosecond jitter allows for synchronizing multiple pulse generators to form a high power array. The closed loop timing and synchronization control system is described in this section.

A block diagram of the timing and synchronization control system is shown in Figure 9. Although only two pulse generator modules are shown in the block diagram, the control system could be expanded to a larger number of units. The control system is based on using a National Instruments (NI) PXI-1042 chassis which houses a PXI-8196 embedded controller, a PXI-6653 timing and multi-chassis synchronization module, a PXI-7831R reconfigurable input/output (RIO) card, an Agilent (formerly Acqiris) DC140 PXI digitizer card, and has a resistive touch panel human machine interface (HMI).

A Highland Technology P400 digital delay generator is used to drive each trigger pulser. One channel of the P400 is set as the reference and the relative delay of the other channel is adjusted to synchronize the outputs.

The output of each main Marx pulse generator is monitored using D-dot probes attached to the output coaxial cables. Analog to digital conversion (ADC) of the D-dot probe outputs is accomplished using the DC140 PXI digitizer card. A random interleaved sampling (RIS) scheme allows for over-sampling of the D-dot probe output at a rate of >20 Gs/s. This over-sampling rate allows for time resolution of the analog signals to <50 ps which is more that adequate for synchronization of multiple Phase II Marx generator modules.

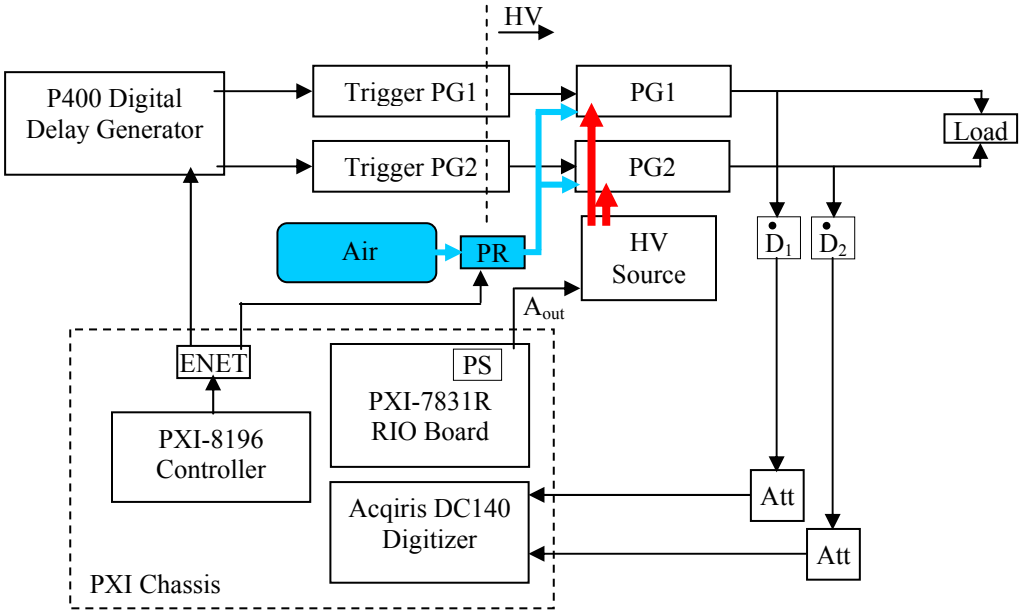

Figure 9. Timing and synchronization control system.

The outputs of the digitizer card are analyzed in LabVIEW code to find the peak in the D-dot probe outputs and determine the appropriate delays for the trigger pulsers. After the delays are calculated, the system controller communicates with the P400 digital delay generator via Ethernet to set the appropriate delays between channels. The P400 is also used as the rate generator and sets the pulse repetition rate.

If desired, the control system can monitor atmospheric pressure and adjust the Marx generator pressure and input voltage to maintain the desired output voltage magnitude. This mode of operation could be used on an air-mobile platform or in those cases where the unit is transported through various elevations. The electronic pressure regulator communicates with the control system via Ethernet and the output of the high voltage capacitor charging power supply is controlled using an analog output of the RIO board.

VI. TEM HORN ANTENNA

A TEM horn antenna, shown in Figure 10, was fabricated to be used with the Phase II Marx generator in order to provide a complete high power impulse source. The TEM horn is an unbalanced design having a tapered horn section cantilevered above a ground plane. Other basic design constraints were that the antenna should be compact and transportable, be easily assembled and mounted, have the largest radiating aperture practicable, and be designed for operation at high voltages and high peak power levels.

The ground plane size was set at 4x10 ft and was fabricated by laminating aluminum sheet to a composite substrate. The height of the aperture was set at 32 inches above the ground plane giving a width to height ratio of 1.5. Choosing a desired characteristic impedance of Z_c = 200 Ω, design guidance [4] was referenced to determine the angular width of the triangular section (α) and the angular separation between the triangular section and ground plane (β/2) of 25° and 16.5°, respectively. TDR was used to characterize the horn impedance which measured close to that predicted by theory.

Figure 10. TEM horn antenna.

VII. REFERENCES

[1] S. J. MacGregor, et al., "Factors Affecting and Methods of Improving the Pulse Repetition Frequency of Pulse-Charged and DC-Charged High-Pressure Gas Switches," IEEE Trans. Plasma Science, **25**, 110-117 (1997).

[2] C. E. Baum and J. M. Lehr, "Charging of Marx Generators," CESDN 43, AFRL/DEHP (2000).

[3] J. O'Loughlin, et al., "High Repetition Rate Charging a Marx Type Generator," in Conference Record of the Pulsed Power and Plasma Science Conference (2001).

[4] R. Todd Lee, and Glenn S. Smith, "On the Characteristic Impedance of the TEM Horn Antenna," IEEE Trans. Antennas and Propagation, **52**, 315-318.